ASTRONOMY & ASTROPHYSICS
SUPPLEMENT SERIES

OCTOBER II 1990, PAGE 895

Astron. Astrophys. Suppl. Ser. **85**, 895-913 (1990)

Dust in emission nebulae of the LMC derived from photometric reddening of stars(*)

A. Greve(1), A.M. van Genderen(2) and A. Laval(3)

(1) IRAM, 300 Rue de la Piscine, Domaine Universitaire, 38406 St. Martin d'Heres, France
(2) Sterrewacht Leiden, Huygens Laboratorium, Wassenaarseweg 78, 2300 RA Leiden, The Netherlands
(3) Observatoire de Marseille, 2 Place Le Verrier, 13248 Marseille Cedex 04, France

Received January 29, accepted March 22, 1990

Abstract. — We present *VBLUW* photometric observations of stars in emission nebulae of the LMC (N 4AB, N 11AB, N 12, N 48ACB, N 57C, N 77, N 79ABDE, N 81, N 83AB, N 163, N 195, N 214C, 30 Dor). The luminosities and extinctions A_V of the stars are derived. We find agreement between the average photometric extinctions of the nebulae and the extinctions derived from the Balmer line decrement measured by Caplan and Deharveng (1985, 1986). The photometric extinctions are shown in the CO map of the LMC (Cohen *et al.*, 1988).

Key words: LMC — emission nebulae — stars — photometry — extinction.

1. Introduction.

In an earlier publication (Greve *et al.*, 1988 ; Paper I) we derived representative average reddenings of emission nebulae (EN) in the SMC and LMC from Walraven *VBLUW* photometric observations of embedded stars. In a similar way, the photometric observations reported here concentrate on stars in EN of the LMC of which the Balmer decrements (integrated over 4.89' diameter areas) measured by Caplan and Deharveng (1985, 1986 ; abbreviated CAD) deviate significantly from the theoretical value predicted from case B recombination line model calculations (cf. Osterbrock, 1974). The observed deviations of the Balmer decrement may result from extinction in more or less uniformly screening dust. When adopting this interpretation, the question arises whether there exists agreement between the extinctions derived from the stellar photometry and the Balmer decrement method, as suggested by CAD to be the case. The investigation of this question is important since the Balmer decrement method is frequently used to derive extinction in extragalactic systems. There are indications that the recombination case B may not be generally applicable for extragalactic H II regions (Ward *et al.*, 1987 ; Rieke and Lebofsky, 1981).

The dust component of the nebulae, evident as optical extinction, may be related to associated CO clouds detected by Israel *et al.* (1982, 1986) and Cohen *et al.* (1988), and recently being investigated in more detail with SEST (Booth *et al.*, 1989, Johansson *et al.*, 1988).

(*) Based on observations collected at ESO, La Silla, Chile.

2. Observations and reductions.

The observations were made January 1989 using the Walraven *VBLUW* photometer (Walraven and Walraven, 1960 ; Rijf *et al.*, 1969 ; Lub and Pel, 1977) attached to the 90 cm Dutch telescope at the European Southern Observatory (ESO), Chile. The reduction of the observations follows the procedure explained in Paper I.

The EN were selected from the objects observed by CAD, and are identified by the numbers of Henize's catalogue (1956). The observed stars are identified in Figures 1.1–1.13 ; the corresponding *VBLUW* data for the photometric system in use since 1980 are given in Table I.a–I.s. The apparent visual magnitudes V_J (*not* corrected for reddening) in the *UBV* system (with quantities of the *UBV* system denoted by the index J) are derived from relation (1) (Pel, 1987)

$$V_J = 6.889 - 2.5\ [V + 0.033\,(V - B)] \qquad (1)$$

The *VBLUW* data are logarithm of intensity, the *UBV* data are given in units of magnitudes.

Reddening corrected absolute visual magnitudes M_{VJ} are calculated for a distance modulus of 18.6.

Our criterion for the membership of the stars with the EN is their location in/or proximity to these objects. Stars identified from the *VBLUW* measurements as Galactic foreground stars are indicated as such in Table I (with deduced spectral types given in brackets).

Figure 2 shows the stars in the $V - B/B - L$ colour diagram of the Walraven system. The main sequence (ms) is inserted. The majority of the LMC stars are OB ms stars. For very bright objects we cannot exclude the possibility of being unresolved groups of (blue) stars or bright WR and Of stars (Rosado, 1986; for absolute magnitudes of Of stars see Feinstein *et al.*, 1986). Notes on individual objects are given in Section 7.

For several objects we have measured the nebular emission. The data are given in Table II, the positions of the observations are shown in Figure 1, and the colours are displayed in Figure 2. The colours agree with earlier observations of EN published by Greve and van Genderen (1987).

For several stars the observed colours are contaminated by nebular emission entering the 16" diameter diaphragm. In the colour diagram of Figure 2, these stars are located above the reddening line of OB ms stars. The stars with pronounced contamination by nebular emission were corrected either by taking into account the measured nebular background, or were tentatively identified as OB ms stars and shifted to the OB ms star reddening line along the empirically determined direction of nebular contamination $\delta\,(B - L)/\delta\,(V - B) \sim 1$, $\delta\,(B - U)/\delta\,(V - B) \sim 0.8$ in the $V - B/B - L$ and $B - U/V - B$ colour diagrams, respectively. Stars with values $E(V - B)$, A_{vJ}, $(B - V)_{J0}$ and M_{vJ} derived by applying these corrections are indicated by $ in Table I.

3. Photometric extinction.

The extinctions A_{vJ} are derived by moving the stars along the reddening lines to the ms or supergiant branch which in this region of the colour diagram is located slightly to the right side of the ms. This procedure gives the values $E(V - B)$ listed in Table I. The corresponding values $E(B - V)_J$ are derived from relation (2) (Pel, 1987)

$$E(B - V)_J/E(V - B) = 2.39 - 0.17E(V - B) \quad (2)$$

Finally, $A_{vJ} = R\,E(B - V)_J$. We have used $R = 3.3$ and the standard Galactic reddening curve (cf. Savage and Mathis, 1979) which may be applied to the LMC in the wavelength region of the photometric observations (Mathis *et al.*, 1985; Koornneef, 1982; Morgan and Nandy, 1982; Clayton and Martin, 1984). We have used $R = 3.3$ as applied by Lub and Pel (1977) for the determination of reddening in the *VBLUW* system. With respect to the standard value $R = 3.1$, the value $R = 3.3$ introduces a difference in A_{vJ} of ~6%. We are unable to distinguish between foreground extinction in the LMC, absorbing material around the EN, extinction in the nebulae, and absorbing material around the stars.

The observations listed in Table I and Table II are *not* corrected for Galactic extinction in the direction of the LMC (see section 6).

Our observations are biased towards low extinction; high extinction is only detected in case the stars are sufficiently bright ($V_J < 16$ mag.) to be located with the telescope. Figure 3 shows the reddening corrected luminosities M_{vJ} and extinctions A_{vJ} observed in the directions of the stars. This figure suggests that the more luminous objects are located in the regions of higher extinction.

4. HR diagram.

The reddening corrected values $(V - B)_0$ are obtained from $E(V - B)$ by $(V - B)_0 = (V - B) - E(V - B)$. The colours $(B - V)_{J0}$ are derived from $(V - B)_0$ using relation (3) (Pel, 1987)

$$(B - V)_{J0} = 2.571(V - B)_0 - 1.020\,(V - B)_0^2 + 0.500\,(V - B)_0^3 - 0.010\,\text{(mag)} \quad (3)$$

Figure 4 shows the HR diagram which exhibits ms stars and a few evolved stars. When compared with the isochronous lines of young Galactic clusters (Mermilliod, 1981a, b), the ages of the observed LMC stars are found to be 3-10 $\times$ 10^6 years. Some of the objects brighter than $M_{vJ} \sim -7$ mag. may be unresolved groups of blue stars or single bright WR and Of stars.

5. Comparison of photometric and spectroscopic extinction determinations.

Table III gives for each nebula the average $< A_{vJ} >$ of the individual stellar extinctions, assumed to represent the average extinction of the EN. Table III also gives the number N of stars used to determine the average, and the highest extinction A_{vJ} (max) observed in the nebulae. For N 103 and 30 Dor the average is based on 3, 2 stars respectively so that the quoted $< A_{vJ} >$ (:) must be taken with caution. The values of Table III are *not* corrected for Galactic foreground extinction.

Under the assumption that the dust is uniformly distributed, the observed $R_0 = F(\text{H}\alpha)/F(\text{H}\beta)$ and predicted $R_p = I(\text{H}\alpha)/I(\text{H}\beta)$ Balmer decrement may be used (Mathis, 1983; CAD) to derive the extinction

$$A_{vJ}\,(\alpha/\beta) = 6.83\,\log\,(R_0/R_p)\ \text{(mag)} \quad (4)$$

$R_0 = 2.86$ for recombination case B (cf. Osterbrock, 1974). The factor 6.83 is calculated for the Galactic reddening curve and $R = 3.3$ as used for the reduction of the photometric observations. The values $A_{vJ}(\alpha/\beta)$ derived from the Hα, Hβ observations by CAD are given in Table III. For several EN additional spectroscopic observations of Hα and Hβ line fluxes are available in the literature, however, these observations usually cover only the brighter parts of the nebulae. From the published parameters $c(\text{H}\beta)$ (see Kaler, 1976) the extinctions A_{vJ} (sp)= 2.40 $c(\text{H}\beta)$ are derived using the Galactic reddening curve and $R = 3.3$. The values A_{vJ} (sp) are given in Table III. This table also gives the extinctions A_{vJ} (L) derived by Lucke (1972) from photometric observations of stars associated with the EN or located in their vicinity.

The corresponding values $E(B-V)_J$ derived by Lucke are compiled by Braunsfurth and Feitzinger (1983), and $R = 3.3$ was used as before.

The stars observed by us are confined to the areas of the EN measured by CAD. Despite the selective nature of the photometric observations the data of Table III indicate agreement between the photometric, $< A_{vJ} >$, and spectroscopic, $A_{vJ}(\alpha/\beta)$, extinctions. The correlation of $< A_{vJ} >$ and $A_{vJ}(\alpha/\beta)$ is shown in Figure 5. The deviation in the correlation for $A_{vJ} > 1$ mag. is probably due to a selection effect in the photometry concentrating on stars located in/or close to the EN.

We conclude that the stellar photometry and wide field Hα-Hβ spectroscopy by CAD probe the same dust component located in and/or around the EN. There exists spatial non-uniformity of the dust distribution as evident from the individual values A_{vJ} of Table I ; however, a possible clumpiness of the dust seems not to destroy the agreement between $< A_{vJ} >$ and $A_{vJ}(\alpha/\beta)$. The non-uniformity of the dust distribution may explain the scatter in Figure 5. However, the correlation displayed in this figure may be fortuitous because the selection effects of both observational methods are difficult to assess.

6. Distribution of the photometric extinction in the LMC.

The determination by Schwering (1988) of the Galactic foreground extinction across the LMC from IRAS observations may be used to correct the reddening values of Table III. Although the Galactic foreground extinction varies across the LMC, we adopted the value $E(B-V)_J = 0.07$, i.e. $A_{vJ} = 0.23$ mag. with an estimated uncertainty for the individual nebulae of ± 0.02 in $E(B-V)$, i.e. ± 0.07 in A_{vJ}.

The foreground corrected extinctions $< A_{vJ} >_c = < A_{vJ} > -0.23$ mag.are shown in Figure 6 superimposed on the CO emission detected by Cohen *et al.* (1988). The extended, isolated CO clouds outside the 30 Dor region and the bar do not contain conspicuous dark nebulae (Hodge, 1972 ; van den Bergh, 1974), so that possibly no substantial amount of dust has escaped the photometric and spectroscopic observations. Figure 6 shows that the extended, isolated CO clouds contain EN with average extinctions $< A_{vJ} >$ 0.3 – 0.4 mag. The giant CO cloud of the 30 Dor region, however, contains EN (for instance N 159, N 160) with average extinctions $< A_{vJ} > \sim 1.0 - 1.5$ mag., and large, opaque dark nebulae are evident in this region.

7. Notes on individual objects.

N 4 AB

Object 2 (number 1 in Fig. 2) is identified as a star, the colours are contaminated by nebular emission. Object 3 is a cluster of 3 stars embedded in nebulosity. When corrected for nebular emission, the colours of object 4 indicate a supergiant of type A.

N 11A

This object is a compact, highly excited H II region of $A_{vJ} = 0.6$ mag. extinction as derived from spectroscopic observations (Heydari-Malayeri and Testor, 1983, 1985). Although the extinction is low, no star is detected in the photometric measurements and the observed colours are typical of nebular emission. A central star therefore must have a brightness $M_{vJ} > -4.7$ mag.

N 11B

Object 3 has peculiar, red colours (see Fig. 2). When compared with the *VBLUW* observations of planetary nebulae (Greve and van Genderen, 1987), this object is tentatively identified as such. The apparent brightness $V_J = 12.8$ may contradict this identification (Westerlund and Smith, 1964). The lists of planetary nebulae published by Lindsay and Mullan (1963), Westerlund and Smith (1964), Sanduleak *et al.* (1978), and Sanduleak and Philip (1977) do not contain this object. The red colour of this object is confirmed by B and V CCD images (Testor, priv. comm.). Object 3 is object 529 of Woolley's (1963)investigation with $V_J = 12.2$ and $(B-V) = 3.01$ (:). Using relation (3) we derive $(B-V)_J = 1.64$. This object merits further spectroscopic and IR observations.

Object 10 (number 2 in Fig. 2) is object number 4 of the investigation by Heydari-Malayeri and Testor (1985) and is identified as an excited condensation similar to N 11A, with no visible stellar component. The observed *VBLUW* colours of this object are similar to those of nebular emission. The colours and apparent brightness of object 11 (number 3 in Fig. 2) are similar to those of object 10. We tentatively identify this object as another excited condensation. Both objects, 10 and 11, are located at the edge of an emission line ridge near the eastern rim of N 11B (see Fig. 1.2). Object 11 merits further observations. Object 13 is object number 2 of the investigation by Heydari-Malayeri and Testor (1985), also identified as an excited condensation with SK 6637 the central star. Contrary to object 10 and 11, the nebular emission of object 13 is weak since the observed *VBLUW* colours are those of a star.

The stars 13, 14, 18, 19, 25, 26 were observed with the intention to search for extinction outside the body of nebular emission. The highest extinction is observed for the stars 15 and 18 lying outside the EN.

The average extinction of N 11B, excluding stars outside the emission region, is $< A_{vJ} > = 0.77$ mag. The stars 21, 22, 23, 24 belong to the cluster located in the western part of N 11B. The average extinction in the cluster region is $< A_{vJ} > = 0.98$ mag.

N 48AC

Star 1 is very bright, possibly being a stellar cluster. However, the possibility of being a single bright WR or Of star can not be excluded.

Object 5 (number 4 in Fig. 2) has somewhat peculiar colours. This object appears as two close stars in Hodge and Wright's (1967) atlas of the LMC.

N 48B

Object 41 has peculiar, red colours (see Fig. 2). When compared with the *VBLUW* observations of planetary nebulae (Greve and van Genderen, 1987), this object is tentatively identified as such. The apparent brightness $V_J =$ 13.8 may contradict this identification (Westerlund and Smith, 1964). The lists of planetary nebulae published by Lindsay and Mullan (1963), Westerlund and Smith (1964), Sanduleak *et al.* (1978), and Sanduleak and Philip (1977) do not contain this object. The object merits further spectroscopic and IR observations.

N 79D

Object 15 (number 5 in Fig. 2) is probably a compact H II region.

N 81, N 83

The stars were selected to coincide with the regions measured by CAD.

N 103

This object is a crowded, compact cluster of which the central stars cannot be separated in the diaphragm. The listed average value $< A_{vJ} >$ has to be taken with caution because of the few observed stars ; however, there exists agreement between $< A_{vJ} >$ and $A_{vJ}(\alpha/\beta)$.

N 163

Object 3 is a stellar-like, peculiar, red object. We were able to measure only $(V-B)$; the other colours are omitted because of poor signal to noise. This object merits further spectroscopic and IR observations.

30 Doradus

The observed stars were selected for comparison of extinction determinations from $P\gamma/H\delta$ and $P\delta/H\epsilon$ ratios measured in a nearby nebular region (Greve *et al.*, 1989a, b).

Conclusions.

The majority of stars associated with the LMC emission nebulae are more or less reddened OB main sequence stars of 3-10 × 10^6 years age.

When assuming uniform distribution of dust in and/or around the emission nebulae, the average photometric extinction agrees (within the limits of the statistical significance of the photometric data) with the corresponding extinctions derived from the Balmer decrement measured by Caplan and Deharveng (1985, 1986). The collected data (reported here and in Paper I) seem to give confidence that the stellar photometric observations and spectroscopic observations of the Balmer decrement by CAD probe the same average amount of dust. The individual values of the stellar photometric extinctions suggest some clumpiness of the dust, however, not affecting the agreement between the average extinctions obtained from both observational methods.

The photometric extinctions are shown superimposed on the CO map of the LMC published by Cohen *et al.* (1988). Isolated CO clouds seem to contain emission nebulae with extinctions $A_{vJ} \gtrsim 0.4 - 0.5$ mag., whereas the extinction of emission nebulae (N 159, N 160) in the 30 Dor region is $A_{vJ} \sim 1.0 - 1.5$ mag.

Acknowledgements.

We appreciated the assistance of Mr. Th. Augusteijn and Dr. H.E. Schwarz (ESO, La Silla) during the preliminary data reduction, and we appreciated the comments of the referees, Dr. F. Israel and Prof. J. Lequeux.

References

BOOTH R.S., DELGADO G., HAGSTROM M., JOHANSSON L.E.B., MURPHY D.C., OLBERG M., WHYBORN N.D., GREVE A., HANSSON B., LINDSTROM C.O., RYDBERG A.: 1989, *Astron. Astrophys.* **216**, 315.
BRAUNSFURTH E., FEITZINGER J.V.: 1983, *Astron. Astrophys.* **127**, 113.
CAPLAN J., DEHARVENG L.: 1985, *Astron. Astrophys. Suppl. Ser.* **62**, 63.
CAPLAN J., DEHARVENG L.: 1986, *Astron. Astrophys.* **155**, 297 (CAD).
CLAYTON G.C., MARTIN P.G.: 1984, *IAU Symp.* **108**, (Reidel, Dordrecht) p. 403.
COHEN R.S., DAME T.M., GARAY G., MONTANI J., RUBIO M., THADDEUS P.: 1988, *Astrophys. J.* **331**, L 95.
DICKEL H.R., ALLER L.H., FAULKNER D.J.: 1964, *IAU Symp.* **20**, p. 294.
DUFOUR R.J.: 1975, *Astrophys. J.* **195**, 315.
FEINSTEIN A., VASQUEZ R.A., BENVENUTO O.G.: 1986, *Astron. Astrophys.* **159**, 223.
GREVE A., VAN GENDEREN A.M.: 1987, *Astron. Astrophys.* **174**, 243.
GREVE A., VAN GENDEREN A.M., LAVAL A., VAN DRIEL W., PREIN J.J.: 1988, *Astron. Astrophys. Suppl. Ser.* **74**, 167 (Paper I).
GREVE A., MCKEITH C.D., CASTLES J.: 1989a, *ESO Messenger* **57** (Sept.) 56.
GREVE A., MCKEITH C.D., BARNETT E.W., GOTZ M.: 1989b, *Astron. Astrophys.* **215**, 113.
HENIZE K.G.: 1956, *Astrophys. J. Suppl. Ser.* **2**, 315.
HEYDARI-MALAYERI M., TESTOR G.: 1983, *Astron. Astrophys.* **118**, 116.

HEYDARI-MALAYERI M., TESTOR G.: 1985, *Astron. Astrophys.* **144**, 98.
HODGE P.W.: 1972, *Publ. Astron. Soc. Pacific* **84**, 365.
HODGE P.W., WRIGHT F.W.: 1967, The Large Magellanic Cloud, Smithsonian Inst. Astrophys. Obs. (Smithsonian Press).
ISRAEL F.P., DE GRAAUW Th., LINDHOLM S., VAN DER STADT H., DE VRIES C.P.: 1982, *Astrophys. J.* **262**, 100.
ISRAEL F.P., DE GRAAUW Th., VAN DER STADT H., DE VRIES C.P.: 1986, *Astrophys. J.* **303**, 186.
ISSERSTEDT J.: 1975, *Astron. Astrophys.* **41**, 175.
JOHANSSON L.E.B., BOOTH R.S., MURPHY D.M., OLBERG M.: 1988, Submillimeter and Millimeter Astronomy, Kona Conf., Hawaii, Kluwer Academic Publ.
KALER J.B.: 1976, *Astrophys. J. Suppl. Ser.* **31**, 517.
KOORNNEEF J.: 1982, *Astron. Astrophys.* **107**, 247.
LINDSAY E.M., MULLAN D.J.: 1963, *Irish Astron. J.* **6**, 51.
LUB J., PEL J.W.: 1977, *Astron. Astrophys.* **54**, 137.
LUCKE P.B.: 1972, Thesis (Univ. Washington).
MATHIS J.S.: 1983, *Astrophys. J.* **267**, 119.
MATHIS J.S., CHU Y-H., PETERSON D.E.: 1985, *Astrophys. J.* **292**, 155.
MERMILLIOD J.: 1981a, *Astron. Astrophys.* **97**, 235.
MERMILLIOD J.: 1981b, *Astron. Astrophys. Suppl. Ser.* **44**, 467.
MORGAN D.H., NANDY K.: 1982, *Mon. Not. R. Astron. Soc.* **199**, 979.
OSTERBROCK D.E.: 1974, Astrophysics of Gaseous Nebulae, Freeman, San Francisco.
PEIMBERT M., TORRES-PEIMBERT S.: 1974, *Astrophys. J.* **193**, 327.
PEL J.W.: 1987, Intern. Report, Leiden Observatory.
RIEKE G.H., LEBOFSKY M.J.: 1981, *Astrophys. J.* **13**, 157.
RIJF R., TINBERGEN J., WALRAVEN Th.: 1969, *Bull. Astron. Inst. Neth.* **20**, 279.
ROSADO M.: 1986, *Astron. Astrophys.* **160**, 211.
SANDULEAK N., PHILIP A.G.D.: 1977, *Publ. Astron. Soc. Pacific* **89**, 792.
SANDULEAK N., MACCONNELL D.J., PHILIP A.G.D.: 1978, *Publ. Astron. Soc. Pacific* **90**, 621.
SAVAGE B.D., MATHIS J.S.: 1979, *Ann. Rev. Astron. Astrophys.* **17**, 73.
SCHWERING P.: 1988, Thesis (Univ. Leiden).
VAN DEN BERGH S.: 1974, *Astrophys. J.* **193**, 63.
WALBORN N.R., BALDES J.C.: 1987, Space Telescope Sci. Inst., Prepint Series 200.
WALRAVEN Th., WALRAVEN J.: 1960, *Bull. Astron. Inst. Neth.* **15**, 67.
WARD M.J., GEBALLE T., SMITH M., WADE R., WILLIAMS P.: 1987, *Astrophys. J.* **316**, 138.
WESTERLUND B.E., SMITH L.F.: 1964, *Mon. Not. R. Astron. Soc.* **127**, 449.
WOOLLEY R.: 1963, *R. Obs. Bull.* **66**, E 276.

TABLE I a (Fig. 1.1).

N 4 AB

Star	V	(V-B)	(B-U)	(U-W)	(B-L)	VJ	E(V-B)	AVJ	(B-V)J0	MVJ
1	-1.920	0.674	0.872		0.678	11.6			foregr. *	(M)
2$	-3.096	0.346	-0.095	-0.001	-0.068	14.6	0.10	0.78	0.59	-4.8
3$	-2.122	0.192	-0.134	0.120	-0.120	12.2	0.17	0.86	0.22	-7.3
4	-2.571	0.118	0.524	0.181	0.159	13.3	0.02	0.17	0.23	-5.5

TABLE I b (Fig. 1.2).

N 11 A (H II region)

Star	V	(V-B)	(B-U)	(U-W)	(B-L)	VJ	E(V-B)	AVJ	(B-V)J0	MVJ
1	-2.409	0.191	-0.197	0.174	-0.179	12.9		(0.6)		-5.7

TABLE I c (Fig. 1.2).

N 11 B

Star	V	(V-B)	(B-U)	(U-W)	(B-L)	VJ	E(V-B)	AVJ	(B-V)J0	MVJ
2	-1.785	0.042	-0.006	0.064	-0.011	11.3	0.13	1.02	-0.21	-8.3
4$	-2.182	0.051	-0.045	0.026	-0.034	12.3	0.14	1.08	-0.20	-7.4
5$	-2.588	0.027	-0.106	0.007	-0.068	13.4	0.01	0.06	0.04	-5.3
6$	-2.061	-0.011	-0.076	-0.001	-0.050	12.0	0.08	0.63	-0.23	-7.2
7$	-2.336	0.004	-0.077	0.028	-0.060	12.7	0.08	0.63	-0.19	-6.5
8$	-2.727	0.112	-0.135	0.123	-0.104	13.7	0.13	1.02	-0.02	-5.9
9$	-2.894	0.064	-0.078	0.095	-0.098	14.1	0.13	1.02	-0.15	-5.5
12$	-3.056	0.118	-0.164	0.075	-0.108	14.5	0.13	1.02	-0.01	-5.1
13	-2.436	-0.020	-0.036	-0.006	-0.040	13.0	0.07	0.56	-0.23	-6.2
14	-3.181	-0.036	-0.027	-0.010	-0.022	14.8	0.05	0.39	-0.22	-4.2
15$	-3.225	0.093	-0.057	0.004	-0.045	14.9	0.16	1.26	-0.14	-5.0
16$	-2.822	0.086	-0.135	0.069	-0.125	13.9	0.11	0.86	-0.04	-5.6
17$	-2.868	0.049	-0.143	0.112	-0.117	14.1	0.07	0.56	-0.05	-5.1
18$	-3.094	0.162	0.005	0.105	-0.006	14.6	0.24	1.88	-0.15	-5.9
19$	-3.355	-0.054	-0.151	(0.128)	-0.140	15.3	0.0	0.0	-0.15	-3.3
20$	-2.881	0.118	-0.190	0.083	-0.149	14.1	0.11	0.86	0.04	-5.4
21$	-2.417	0.024	-0.113	0.017	-0.069	12.9	0.09	0.69	-0.15	-6.4
22	-1.974	0.005	-0.042	-0.052	-0.011	11.8	0.11	0.86	-0.26	-7.7
23	-2.556	0.038	-0.027	-0.039	-0.012	13.3	0.15	1.19	-0.27	-6.5
24$	-2.584	0.066	-0.078	0.017	-0.030	13.3	0.15	1.19	-0.19	-6.5
25	-3.022	-0.133	-0.080	(0.008)	-0.070	14.5	0.0	0.0	-0.37	-4.1
26$	-3.273	0.064	-0.071		-0.083	15.1	0.14	1.08	-0.17	-4.6
3	-2.376	0.796	-0.101	0.508	-0.061	12.8	PLANET. NEB. ?			-5.8
10	-3.029	0.125	-0.399	0.325	-0.344	14.4	COMPACT H II ?			-4.2
11	-3.195	0.088	-0.351	0.252	-0.346	14.9	COMPACT H II ?			-3.7

TABLE I d (Fig. 1.3).

N 12

Star	V	(V-B)	(B-U)	(U-W)	(B-L)	VJ	E(V-B)	AVJ	(B-V)J0	MVJ
1	-2.466	-0.028	-0.078	-0.016	-0.033	13.1	0.06	0.46	-0.22	-6.0
2	-3.048	-0.031	-0.048	-0.069	-0.040	14.5	0.06	0.46	-0.23	-4.6
3	-3.189	0.000	-0.039	-0.065	-0.020	14.9	0.10	0.79	-0.25	-4.5
4	-3.078	0.001	-0.045	-0.010	-0.026	14.6	0.10	0.79	-0.25	-4.8
5	-2.922	-0.003	-0.045	-0.029	0.000	14.2	0.10	0.79	-0.23	-5.2
6	-3.166	-0.003	0.049	-0.011	-0.012	14.8	0.09	0.70	-0.23	-4.5
7$	-3.270	-0.003	-0.122		-0.097	15.1	0.06	0.46	-0.15	-4.0
8	-3.445	-0.028	0.016		0.001	15.5	0.04	0.30	-0.17	-3.4

TABLE I e (Fig. 1.4).

N 48 AC

Star	V	(V-B)	(B-U)	(U-W)	(B-L)	VJ	E(V-B)	AVJ	(B-V)J0	MVJ
1	-2.321	0.186	0.044	0.026	0.021	12.7	0.26	2.04	-0.12	-7.9
2	-2.752	0.001	0.103	0.056	0.015	13.8	0.09	0.69	-0.22	-5.5
3	-2.624	0.049	0.022	0.044	0.016	13.4	0.15	1.19	-0.24	-6.4
4	-3.516	-0.075	0.095		0.029	15.7	0.0	0.0	-0.21	-2.9
5	-3.488	-0.263	-0.103	-0.020	-0.066	15.6				-3.0
6	-3.302	-0.066	0.020	(0.042)	-0.049	15.1	0.03	0.23	-0.26	-3.7
7	-3.591	-0.054	0.129	(0.051)	0.051	15.9	0.0	0.0	-0.15	-2.7
8	-2.309	0.876	0.478		0.483	12.6			foregr. *	(M)
9	-3.154	0.035	0.005	0.027	0.012	14.8	0.14	1.08	-0.25	-4.9
10$	-3.184	-0.012	-0.050	-0.064	-0.094	14.8	0.08	0.63	-0.23	-4.4
11$	-3.227	-0.068	-0.082	-0.026	-0.100	15.0	0.03	0.23	-0.26	-3.8
12	-3.019	-0.099	-0.067	-0.039	-0.062	14.4	0.0	0.0	-0.27	-4.2
13	-1.945	0.472	0.541		0.474	11.7			foregr. *	(K)
14	-2.883	-0.047	-0.094	-0.003	-0.061	14.1	0.05	0.39	-0.25	-4.9
15	-2.567	-0.009	-0.060	0.019	-0.020	13.3	0.08	0.63	-0.22	-5.9
16	-3.371	-0.039	0.090	-0.009	-0.041	15.3	0.03	0.23	-0.18	-3.5
17$	-2.901	-0.004	-0.068	-0.011	-0.058	14.1	0.08	0.63	-0.21	-5.1
18	-2.896	0.290	0.447		0.276	14.1			foregr. *	(G)
19$	-3.458	0.010	-0.090	0.033	-0.095	15.5	0.08	0.63	-0.17	-3.7
20$	-3.103	-0.002	-0.104	0.130	-0.096	14.6	0.08	0.63	-0.20	-4.6
21	-3.372	-0.113	-0.061	-0.022	-0.061	15.3	0.0	0.0	-0.31	-3.3
22	-3.262	-0.062	0.002	-0.019	-0.050	15.0	0.03	0.23	-0.25	-3.8
23	-3.491	-0.098	-0.038	-0.049	-0.072	15.6	0.0	0.0	-0.27	-3.0
24	-2.381	0.277	0.306	0.214	0.250	12.8			foregr. *	(FG)
25	-2.589	0.253	0.300	0.271	0.219	13.3			foregr. *	(FG)
26	-3.235	-0.005	0.022	0.088	-0.003	15.0	0.08	0.63	-0.21	-4.2
*3	-2.329	0.087	0.040	0.058	0.018	12.7	0.18	1.62	-0.30	-7.5

*3 from Paper I

TABLE I f (Fig. 1.4).

N 48 B

Star	V	(V-B)	(B-U)	(U-W)	(B-L)	VJ	E(V-B)	AVJ	(B-V)J0	MVJ
27	-2.947	-0.001	0.032	-0.054	0.000	14.3	0.08	0.63	-0.20	-4.9
28	-3.285	-0.026	0.018	-0.001	0.006	15.1	0.04	0.30	-0.17	-3.8
29	-2.763	0.762			(0.438)	13.7			foregr. *	(M)
30	-3.015	-0.034	-0.026	-0.005	-0.010	14.4	0.05	0.39	-0.22	-4.6
31	-3.103	0.815	0.483	-0.228	0.563	14.6			foregr. *	(M)
32	-3.015	0.218	(0.356)	(0.241)	0.152	14.4			foregr. *	(F)
33	-3.334	-0.041	-0.004	0.039	-0.001	15.2	0.03	0.23	-0.19	-3.6
34	-3.549	-0.387	(0.251)		(0.173)	15.8			foregr. *	(G)
35	-2.720	0.258	0.297	0.267	0.213	13.7			foregr. *	(G)
36	-2.943	-0.005	-0.051	0.088	-0.015	14.2	0.10	0.79	-0.26	-5.2
37	-3.277	0.689				15.0			foregr. *	(M)
38	-3.690	-0.106	-0.080	(-0.122)	-0.081	16.1	0.0	0.0	-0.29	-2.5
39	-3.064	0.299	0.109		0.081	14.5	0.39	3.00	-0.12	-7.1
40	-2.800	-0.020	-0.068	0.004	-0.041	13.9	0.08	0.63	-0.25	-5.3
41#	-2.787	1.071	0.306		(0.262)	13.8				-4.8
42$	-3.453	0.006	-0.135		-0.125	15.5	0.07	0.56	-0.16	-3.7
43	-3.667	-0.128	-0.036		-0.078	16.1	0.0	0.0	-0.36	-2.5
44	-2.949	0.344	0.396		0.220	14.2			foregr. *	(G)
45	-3.720	-0.034	-0.036	(-0.035)	0.009	16.2	0.03	0.23	-0.17	-2.6
46	-3.262	0.230	0.084		0.000	15.0	0.32	2.46	-0.14	-6.1
*1	-3.278	-0.043	-0.024	-0.006	-0.050	15.1	0.05	0.45	-0.27	-3.9

*1 from Paper I
planetary nebula [or foreground star (M)]

TABLE I g (Fig. 1.5).

N 57 C

Star	V	(V-B)	(B-U)	(U-W)	(B-L)	VJ	E(V-B)	AVJ	(B-V)J0	MVJ
1	-2.501	-0.020	-0.061	-0.034	-0.030	13.1	0.08	0.63	-0.25	-6.1
2	-3.247	0.451	0.317		(0.462)	15.0			foregr. *	(G)
3	-3.471	-0.067	-0.019	(-0.100)	-0.059	15.6	0.03	0.23	-0.26	-3.2
4	-3.790	0.714				16.3			foregr. *	(M)

TABLE I h (Fig. 1.6).

N 77 ABC

Star	V	(V-B)	(B-U)	(U-W)	(B-L)	VJ	E(V-B)	AVJ	(B-V)J0	MVJ
1	-1.402	0.250	0.358	0.213	0.238	10.4			foregr *.	(F)
2	-2.938	0.006	-0.050	-0.008	-0.012	14.2	0.11	0.86	-0.26	-5.3
3	-3.418	0.058	-0.006	(-0.075)	0.016	15.4	0.16	1.26	-0.24	-4.5
4	-3.161	0.126	(0.396)		0.128	14.8			foregr. *	(A)
5	-2.876	0.001	-0.049	0.033	-0.038	14.1	0.09	0.69	-0.22	-5.2
6	-3.389	-0.061	-0.081	-0.064	-0.073	15.4	0.03	0.22	-0.24	-3.4
7	-2.241	-0.015	-0.062	-0.031	-0.023	12.5	0.09	0.69	-0.26	-6.8
8	-1.969	0.285	0.313		0.250	11.8			foregr. *	(F)

TABLE I i (Fig. 1.7).

N 79 AB

Star	V	(V-B)	(B-U)	(U-W)	(B-L)	VJ	E(V-B)	AVJ	(B-V)J0	MVJ
1$	-2.808	-0.010	-0.077	0.003	-0.060	13.9	0.08	0.63	-0.23	-5.3
2$	-2.398	0.172	-0.191	0.142	-0.166	12.9	0.14	1.08	0.11	-6.8
3$	-3.082	0.113	-0.105	0.006	-0.081	14.6	0.14	1.08	-0.04	-5.1
4$	-3.070	0.087	-0.169	0.125	-0.129	14.6	0.09	0.69	0.01	-4.7
5$	-2.994	0.133	0.029	0.110	-0.058	14.4	0.21	1.65	-0.15	-5.8
6	-1.991	0.248	0.338	0.214	0.231	11.8			foregr. *	(G)
7	-2.626	0.023	-0.054	-0.013	0.006	13.4	0.12	0.93	-0.23	-6.1
8	-2.598	-0.017	-0.056	-0.009	-0.025	13.4	0.09	0.69	-0.27	-5.9
9$	-3.205	-0.051	-0.062	-0.067	-0.072	14.9	0.04	0.30	-0.24	-4.0

TABLE I j (Fig. 1.7).

N 79 D

Star	V	(V-B)	(B-U)	(U-W)	(B-L)	VJ	E(V-B)	AVJ	(B-V)J0	MVJ
15	-3.363	0.248	-0.203	0.250	-0.218	15.3		H II REGION		-3.3
16	-3.063	-0.025	-0.057	-0.041	0.005	14.5	0.06	0.46	-0.21	-4.6
17	-3.143	-0.027	-0.038	-0.083	0.003	14.7	0.05	0.39	-0.20	-4.3

TABLE I k (Fig. 1.7).

N 79 E

Star	V	(V-B)	(B-U)	(U-W)	(B-L)	VJ	E(V-B)	AVJ	(B-V)J0	MVJ
10	-2.235	0.308	0.262	0.318	0.222	12.4			foregr. *	(G)
11	-2.370	-0.017	-0.076	0.007	-0.049	12.8	0.07	0.56	-0.23	-6.4
12$	-2.975	-0.039	-0.123	0.016	-0.094	14.3	0.04	0.30	-0.20	-4.6
13$	-3.322	-0.028	-0.183	(0.15)	-0.164	15.2	0.01	0.05	-0.10	-3.5
14	-2.929	0.005	-0.016	0.051	-0.033	14.2	0.09	0.69	-0.20	-5.1
18$	-2.950	0.009	-0.161	0.106	-0.128	14.3	0.05	0.39	-0.10	-4.7
19	-3.153	-0.040	-0.097	0.013	-0.066	14.8	0.05	0.39	-0.24	-4.2
20$	-2.895	-0.026	-0.114	0.044	-0.083	14.1	0.05	0.39	-0.20	-4.9
21	-2.572	-0.014	-0.040	0.002	-0.019	13.3	0.07	0.56	-0.22	-5.9
22	-2.557	-0.025	-0.066	0.007	-0.036	13.3	0.07	0.56	-0.25	-5.9
23$	-2.938	-0.030	-0.110	0.041	-0.084	14.2	0.05	0.39	-0.21	-4.8

TABLE I l (Fig. 1.8).

N 81 A

Star	V	(V-B)	(B-U)	(U-W)	(B-L)	VJ	E(V-B)	AVJ	(B-V)J0	MVJ
1	-2.804	-0.012	-0.049	0.018	-0.028	13.9	0.09	0.69	-0.25	-5.4
2	-2.845	-0.007	-0.032	-0.006	-0.020	14.0	0.09	0.69	-0.24	-5.3

TABLE I m (Fig. 1.8).

N 81 B

Star	V	(V-B)	(B-U)	(U-W)	(B-L)	VJ	E(V-B)	AVJ	(B-V)J0	MVJ
3	-2.793	-0.005	-0.030	0.019	-0.033	13.9	0.09	0.69	-0.23	-5.4
4	-2.530	0.256	0.287	(0.326)	0.205	13.2			foregr. *	(G)
5	-2.737	-0.029	-0.060	0.012	-0.031	13.7	0.06	0.46	-0.23	-5.4

TABLE I n (Fig. 1.8).

N 83

Star	V	(V-B)	(B-U)	(U-W)	(B-L)	VJ	E(V-B)	AVJ	(B-V)J0	MVJ
3	-3.333	-0.077	-0.086	-0.039	-0.053	15.2	0.03	0.23	-0.29	-3.6
4	-2.907	0.027	-0.038	0.025	-0.031	14.2	0.12	0.93	-0.22	-5.3
5	-2.746	-0.028	-0.052	-0.008	-0.052	13.8	0.06	0.46	-0.22	-5.3
6$	-3.217	-0.009	-0.062	-0.018	-0.048	14.9	0.09	0.69	-0.24	-4.0
7$	-3.051	0.028	-0.099	0.050	-0.050	14.5	0.11	0.86	-0.20	-5.0
8$	-3.206	0.073	-0.047		-0.078	14.9	0.15	1.19	-0.17	-4.9
9	-3.164	0.222	0.279		0.165	14.8			foregr. *	(G)
10$	-3.348	0.008	-0.022		-0.042	15.3	0.09	0.69	-0.20	-4.0

TABLE I o (Fig. 1.9).

N 103

Star	V	(V-B)	(B-U)	(U-W)	(B-L)	VJ	E(V-B)	AVJ	(B-V)J0	MVJ
1	-2.387	-0.002	0.050	-0.010	0.027	12.9	0.06	0.46	-0.15	-6.2
2	-2.738	-0.075	-0.065	0.001	-0.041	13.7	0.02	0.17	-0.26	-5.1
3	-3.088	0.255	0.277		0.197	14.6			foregr. *	(G)
4	-2.662	-0.034	0.003	-0.006	0.003	13.5	0.04	0.30	-0.19	-5.4
5	-2.798	0.159	0.350		0.168	13.9			foregr. *	(F)

TABLE I p (Fig. 1.10).

N 163

Star	V	(V-B)	(B-U)	(U-W)	(B-L)	VJ	E(V-B)	AVJ	(B-V)J0	MVJ
1	-2.591	0.038	-0.010	-0.003	-0.004	13.4	0.13	1.02	-0.22	-6.2
2	-2.661	0.034	-0.016	-0.009	0.002	13.5	0.12	0.93	-0.20	-6.0
3	-2.537	0.989				13.1				-5.5
4	-3.451	0.791				15.4			foregr. *	(M)
5	-3.244	0.038	0.001	0.016	0.014	15.0	0.12	0.93	-0.19	-4.5
6	-3.906	0.045	-0.038		0.061	16.6	0.12	0.93	0.07	-2.9

TABLE I q (Fig. 1.11).

N 195

Star	V	(V-B)	(B-U)	(U-W)	(B-L)	VJ	E(V-B)	AVJ	(B-V)J0	MVJ
1	-2.849	-0.027	-0.071	-0.008	-0.051	14.0	0.07	0.56	-0.25	-5.2
2$	-3.004	0.098	-0.052	0.081	-0.020	14.4	0.16	1.26	-0.13	-5.5
3$	-2.856	0.145	-0.048	0.009	-0.036	14.0	0.19	1.49	-0.07	-6.1

TABLE I r (Fig. 1.12).

N 214 C

Star	V	(V-B)	(B-U)	(U-W)	(B-L)	VJ	E(V-B)	AVJ	(B-V)J0	MVJ
1$	-2.639	0.073	-0.185	0.147	-0.148	13.5	0.08	0.63	-0.01	-5.7
2	-2.280	-0.030	-0.076	-0.023	-0.042	12.6	0.07	0.56	-0.26	-6.6
3$	-2.936	0.022	-0.094	0.014	-0.086	14.2	0.09	0.69	-0.16	-5.1
4$	-2.959	0.018	-0.157	0.068	-0.131	14.3	0.06	0.46	-0.10	-4.8
5$	-3.168	-0.028	-0.168		-0.144	14.8	0.03	0.23	-0.15	-4.0
6	-2.640	0.293	0.326		0.290	13.5			foregr. *	(G)
7$	-2.985	0.007	-0.186	0.156	-0.125	14.3	0.03	0.23	-0.06	-4.5

TABLE I s (Fig. 1.13).

30 Dor

Star	V	(V-B)	(B-U)	(U-W)	(B-L)	VJ	E(V-B)	AVJ	(B-V)J0	MVJ
1$	-1.778	0.136	-0.049	0.064	-0.038	11.3	0.19	1.49	-0.10	-8.8
2$	-1.619	0.141	-0.043	0.020	-0.045	10.9	0.19	1.49	-0.08	-9.2

TABLE II. — *Colours of emission nebulae (per 200 (")^2).*

Object	Pos.	V	(V-B)	(B-U)	(U-W)	(B-L)	VJ
N 4	1	-2.895	0.289	-0.349	0.185	-0.307	14.1
N 4	2	-2.348	0.299	-0.175	0.245	-0.174	12.7
N 4	3	-3.651	0.265	-0.341	0.183	-0.146	16.0
N 11B	1	-3.037	0.217	-0.171	0.274	-0.176	14.5
N 11B	2	-3.011	0.141	-0.219	0.214	-0.209	14.4
N 11B	3	-3.195	0.257	-0.427	0.347	-0.407	14.8
N 11B	4	-3.066	0.187	-0.275	0.266	-0.256	14.5
N 11B	5	-3.212	0.328	-0.475	0.272	-0.400	14.9
N 11B	6	-3.261	0.228	-0.304	0.304	-0.288	15.0
N 11B	7	-3.052	0.320	-0.385	0.227	-0.340	14.5
N 11B	8	-3.209	0.305	-0.255	0.332	-0.264	14.9
N 77	1	-2.440	0.160	-0.222	0.215	-0.185	13.0
N 79	1	-2.474	0.166	-0.241	0.295	-0.238	13.1
N 79	2	-3.647	0.057	-0.306		-0.288	16.0
N 195	1	-3.462	0.114	-0.274	0.204	-0.281	15.5
N 195	2	-3.669	0.134	-0.151	0.116	-0.039	16.0
N 195	3	-3.067	0.033	-0.234	0.186	-0.196	14.5
N 214C	1	-3.114	0.135	-0.295	0.369	-0.270	14.7
N 214C	2	-2.919	0.062	-0.086	0.102	-0.091	14.2
N 214C	3	-3.457	0.396	-0.469	0.048	-0.392	15.5

TABLE III. — *Average Extinction (in mag.) of LMC Emission Nebulae (including data of Paper I) (not corrected for Galactic foreground reddening).*

Object	N	A_{VJ}(max)	$<A_{VJ}>$	$A_{VJ}(\alpha/\beta)$	A_{VJ}(L)	A_{VJ}(sp)	Ref.
N 4AB	3	0.8	0.61	0.37	0.36	0.77	1
N 8	4	0.7	0.44			0.38	2
N 9	15	0.5	0.27		0.23	0.38	2
N 11B	18	1.3	0.78	0.48		0.91	2,3
N 11E	3	1.1	0.65	0.48			
N 12	8	0.7	0.60				
N 23A	4	0.5	0.34	0.41	0.20	1.63	2
N 43	8	0.7	0.43		0.40		
N 48AC	21	2.0	0.55	0.82			
N 48B	13	3.0	0.74	0.71			
N 48E	1	1.9					
N 57C	2	0.6	0.42	0.53			
N 59A	17	1.9	0.83	0.87			
N 59B	9	1.4	0.73	0.58		0.89	2,3
N 59C	2	0.7	0.59				
N 63	14	1.2	0.60	0.87	0.82	1.51	2
N 70	30	1.8	0.65			0.67	2
N 77ABC	5	1.3	0.74			0.38	2
N 79AB	8	1.6	0.88	0.83			
N 79D	2	0.6	0.42	0.60	0.40	0.84	1
N 79E	10	0.5	0.42	0.60			
N 81A	2	0.6	0.69	0.72			
N 81B	2	0.6	0.57	0.72	0.70		
N 83	7	1.2	0.72	0.75-0.82		1.15	2
N 84	1	0.5	0.52				
N 103	3	0.4	0.31:	0.30-0.37		0.14	2
N 148GI	9	1.1	0.60	0.46			
N 159A	2	2.3	1.80	1.04-1.14		1.54	4
N 159	20	3.5	1.54	1.06		0.74	1,2
N 160A	15	2.2	1.10	0.79	0.82	0.84	2,3
N 163	4	1.1	0.93	0.91		1.30	2
N 185	8	0.7	0.50				
N 186DC	3	1.6	0.67				
N 195	3	1.5	1.11				
N 214C	6	0.6	0.47	0.41		0.91	3
30 Dor	2	1.5	1.50:	1.39		1.43	5

N	:	number of observed stars
$< A_{vJ} >$	:	average photometric extinction
$A_{vJ}(\alpha/\beta)$	:	extinction derived from Balmer decrement measured by CAD
A_{vJ}(sp)	:	extinction derived from other spectroscopic observations (Ref.)
A_{vJ}(L)	:	extinction derived by Lucke (1972)

1: Peimbert and Torres-Peimbert (1974)
2: Dickel *et al.* (1964)
3: Dufour (1975)
4: Heydari-Malayeri and Testor (1985)
5: Mathis *et al.* (1985), the observed stars are close to their regions III-3 and IV-2 with $c = 0.55$ and $c = 0.64$.

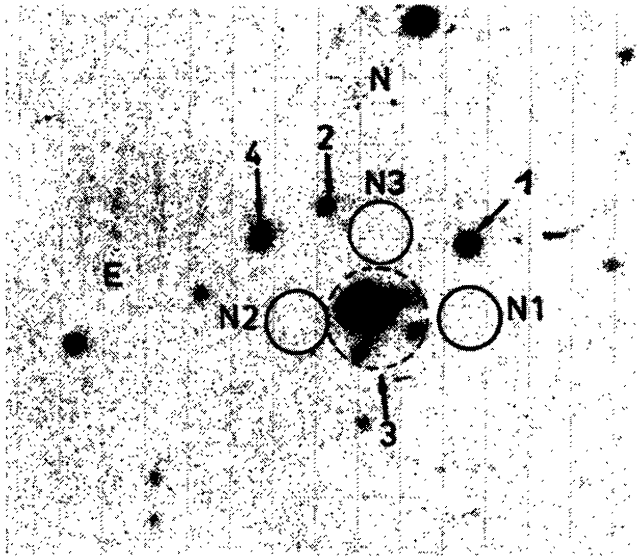

FIGURE 1.1. — N 4 AB (from Hodge and Wright, 1967). The positions of the nebular observations (N) are indicated by the circles.

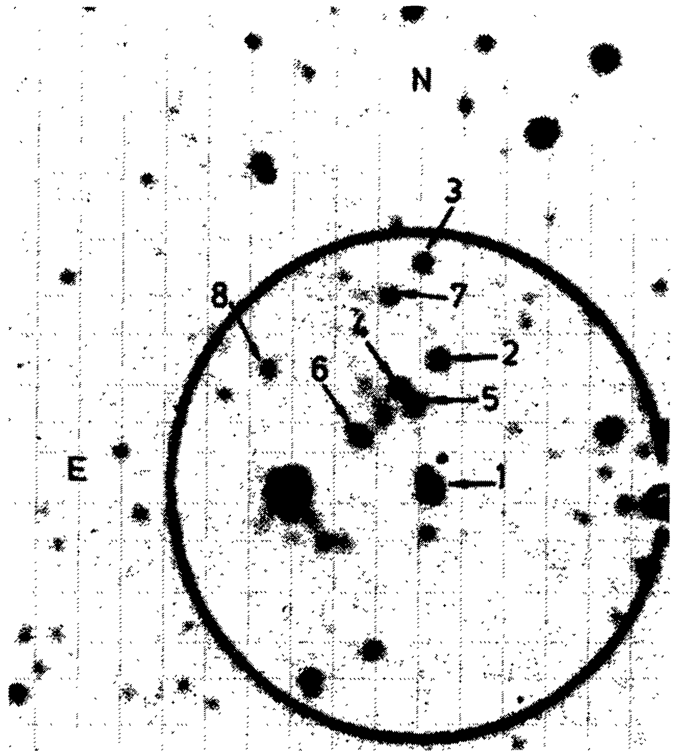

FIGURE 1.3. — N 12 (from Hodge and Wright, 1967).

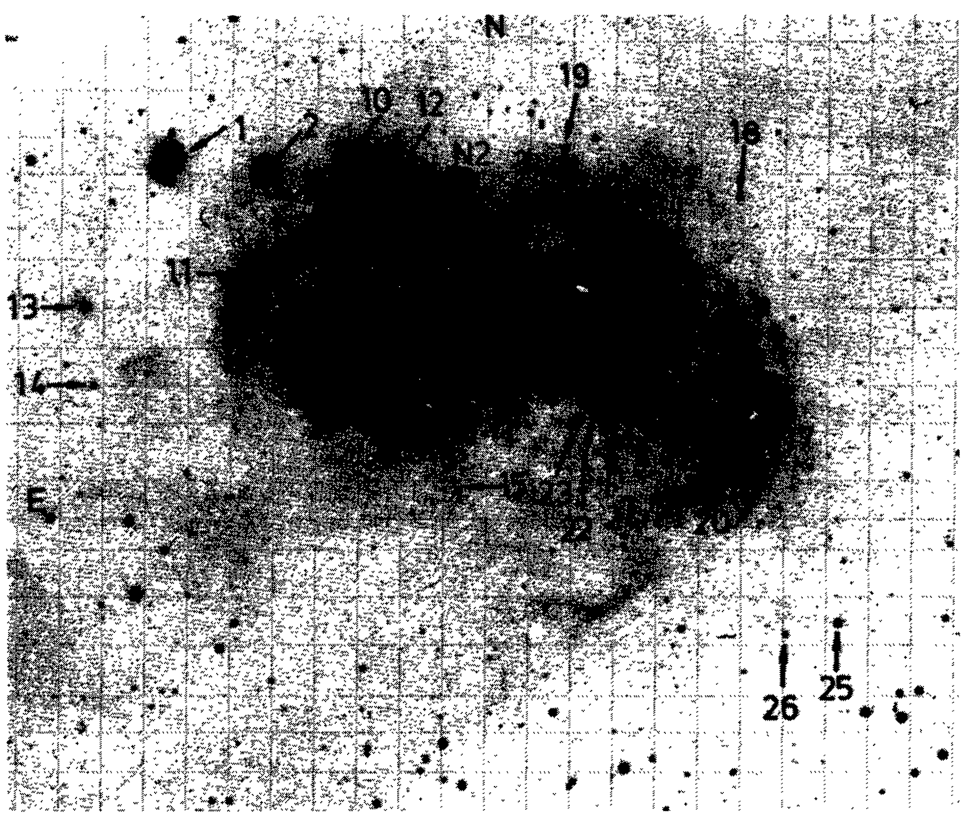

FIGURE 1.2. — N 11 A, N 11 B (plate provided by Dr. G. Testor ; see Heydari-Malayeri and Testor, 1985). The positions of the nebular observations (N) are indicated by the circles.

FIGURE 1.4 — N 48 AC, N 48 B (from Hodge and Wright, 1967). For observations of the stars (1), (2), (3) see Paper I.

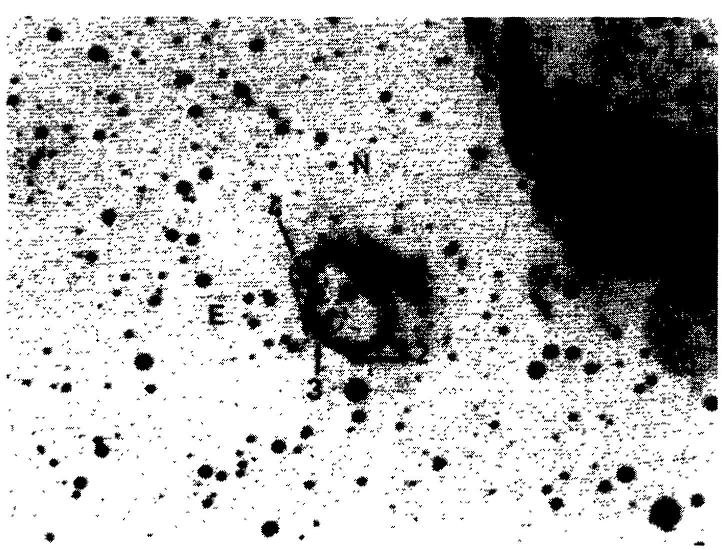

FIGURE 1.5. — N 57 C.

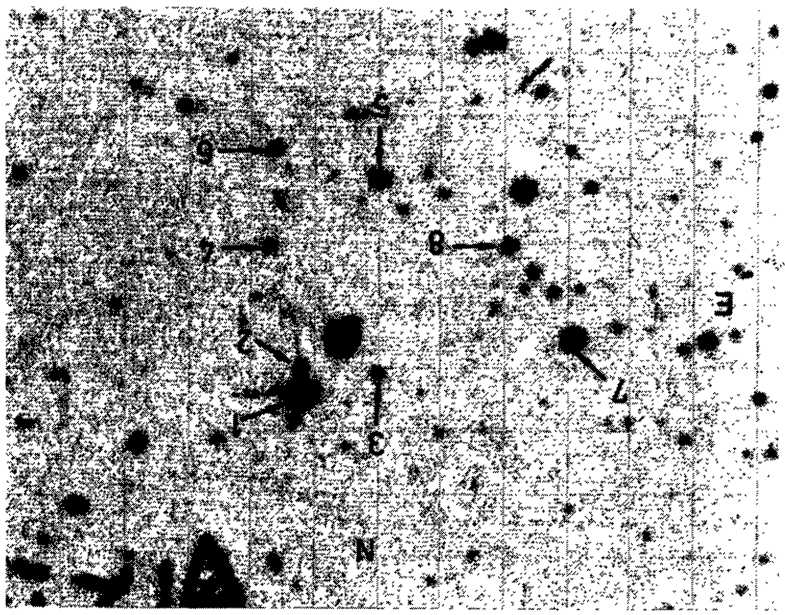

FIGURE 1.6. — N 77 ABC (from Hodge and Wright, 1967).

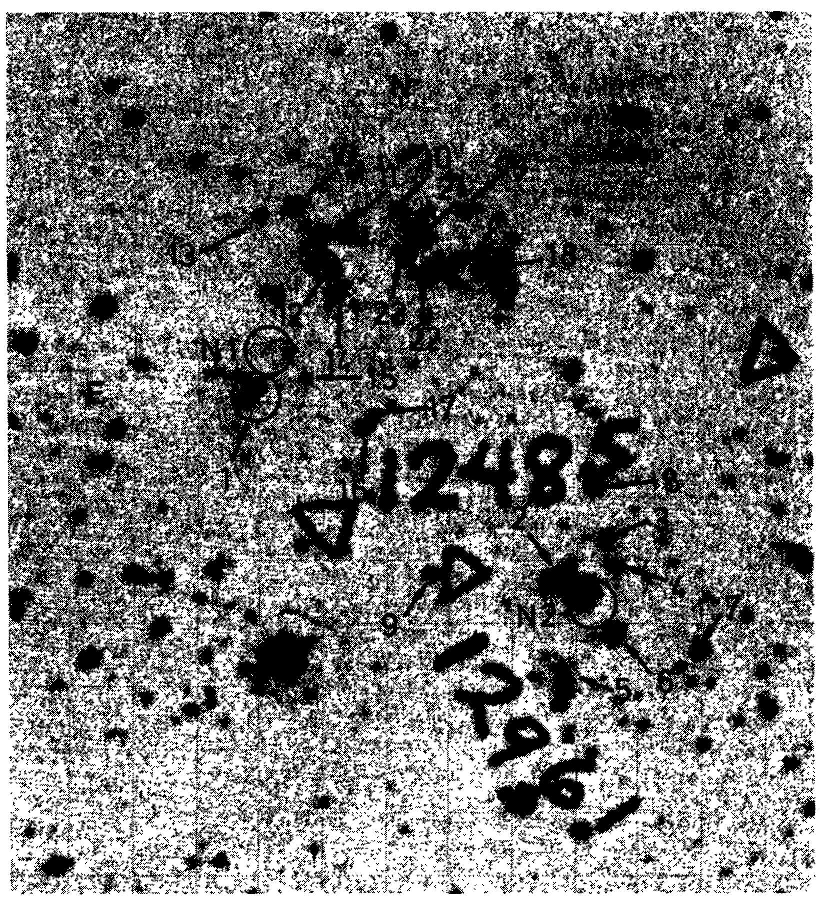

FIGURE 1.7. — N 79 AB, D, E (from Hodge and Wright, 1967). The positions of the nebular observations (N) are indicated by the circles.

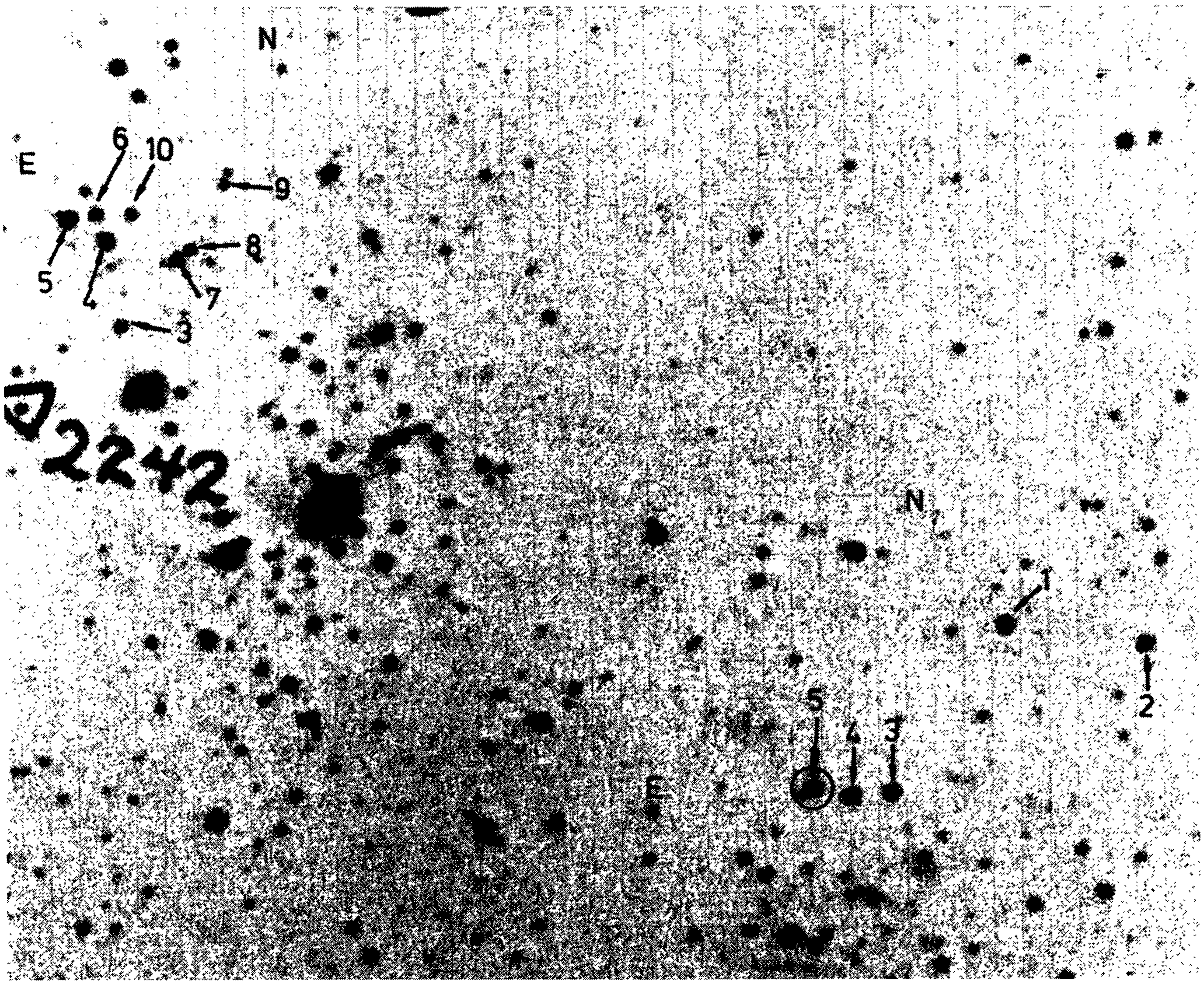

FIGURE 1.8. — N 81 A, B, N 83 (from Hodge and Wright, 1967). The northern association is N 83.

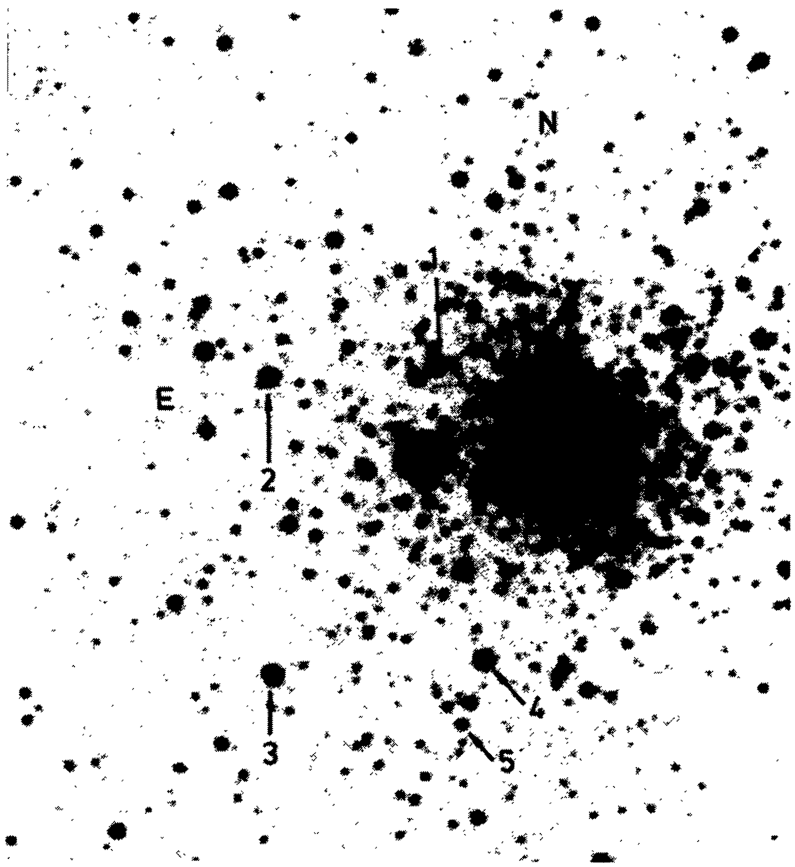

FIGURE 1.9. — N 103.

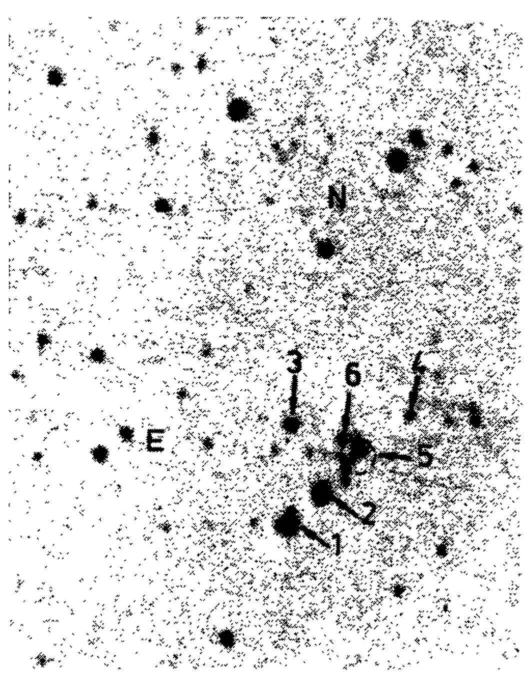

FIGURE 1.10. — N 163 (from Hodge and Wright, 1967).

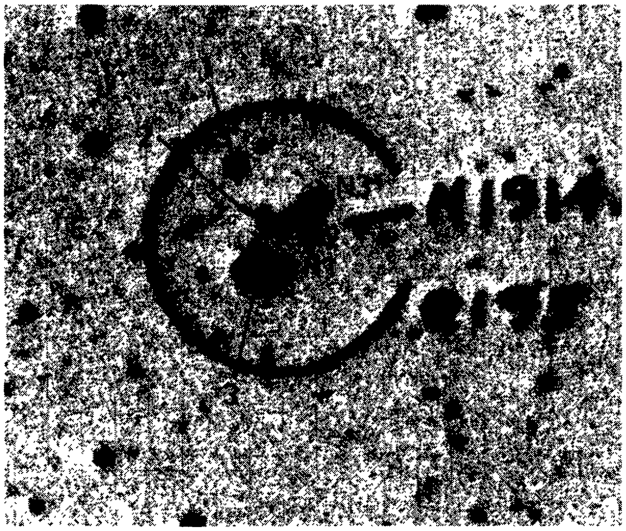

FIGURE 1.11. — N 195 (from Hodge and Wright, 1967). The positions of the nebular observations (N) are indicated by the circles.

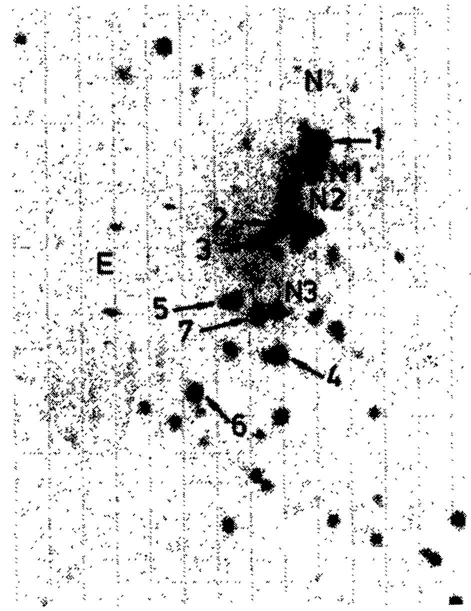

FIGURE 1.12. — N 214 C (from Hodge and Wright, 1967). The positions of the nebular observations (N) are indicated by the circles.

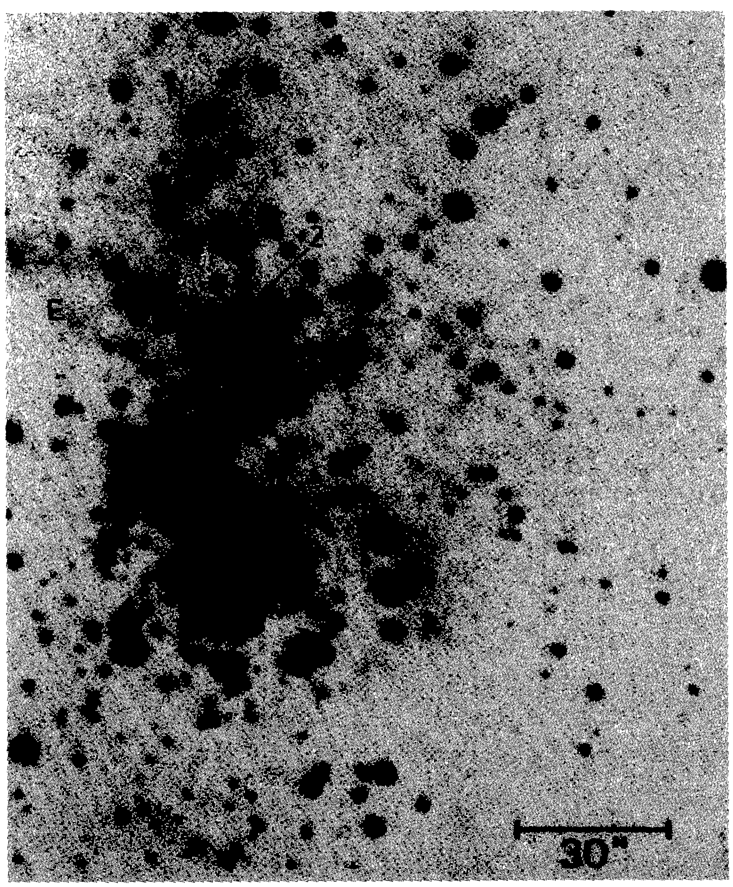

FIGURE 1.13. — 30 Doradus (from Walborn and Blades, 1987).

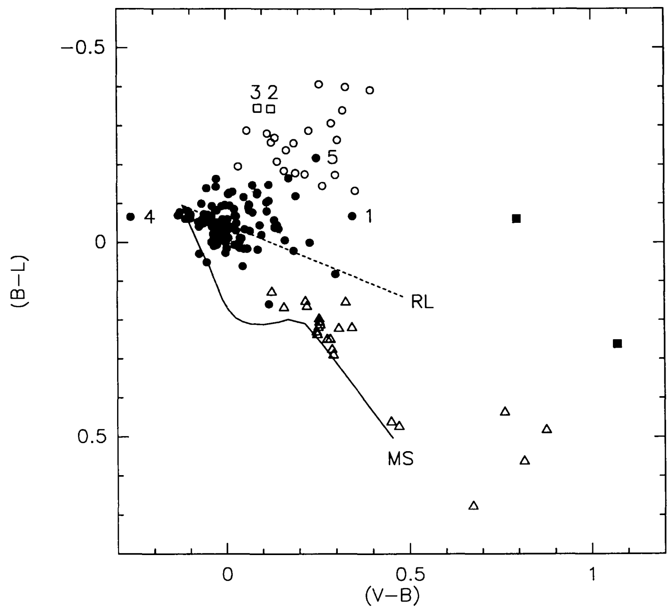

FIGURE 2. — VBLUW colour diagram. LMC stars (•) ; red objects of the LMC (■) (N 11B): object 3, N 48B: object 41); nebular emission (o) ; condensations of N 11B (□) ; Galactic foreground stars (△). The objects denoted by numbers are explained in Section 7. MS: main sequence, RL: reddening line.

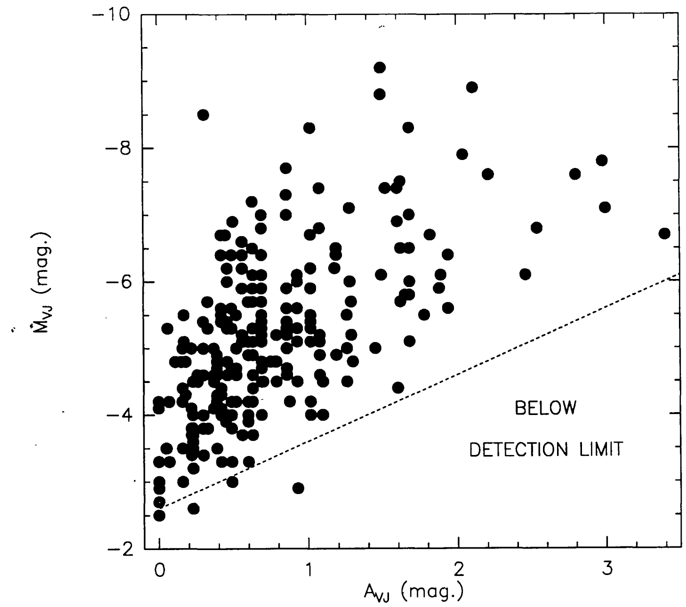

FIGURE 3. — M_{VJ} (reddening corrected) plotted against the extinction A_{VJ} measured in the direction of the stars (data of Paper I included).

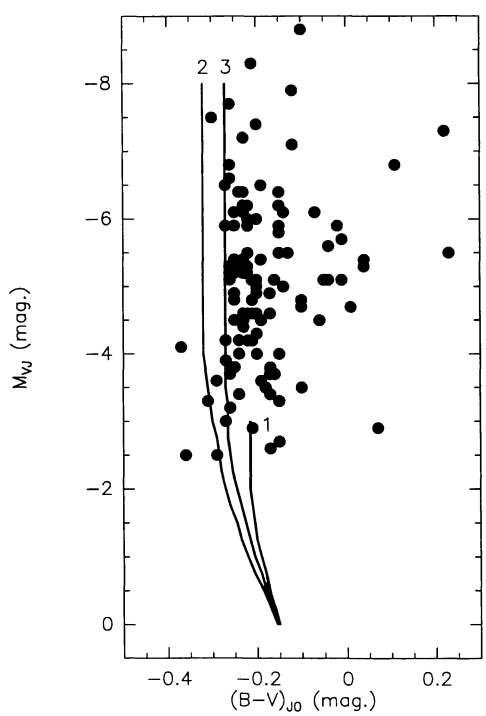

FIGURE 4. — HR diagram of the observed stars and isochronous lines of Galactic clusters taken from Mermilliod (1981a, b). NGC 3766: 1, NGC 6231: 2, NGC 2362: 3.

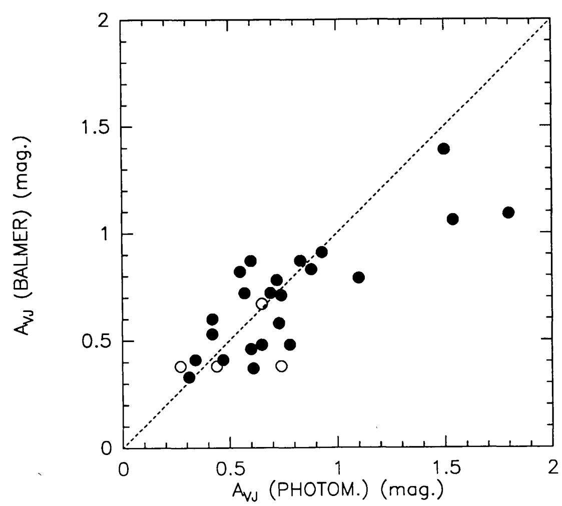

FIGURE 5. — Correlation between average photometric extinction and extinction derived from Balmer decrements measured by CAD (•). The points o denote extinctions derived from other Hα/Hβ observations (Table III). The values are not corrected for Galactic foreground extinction.

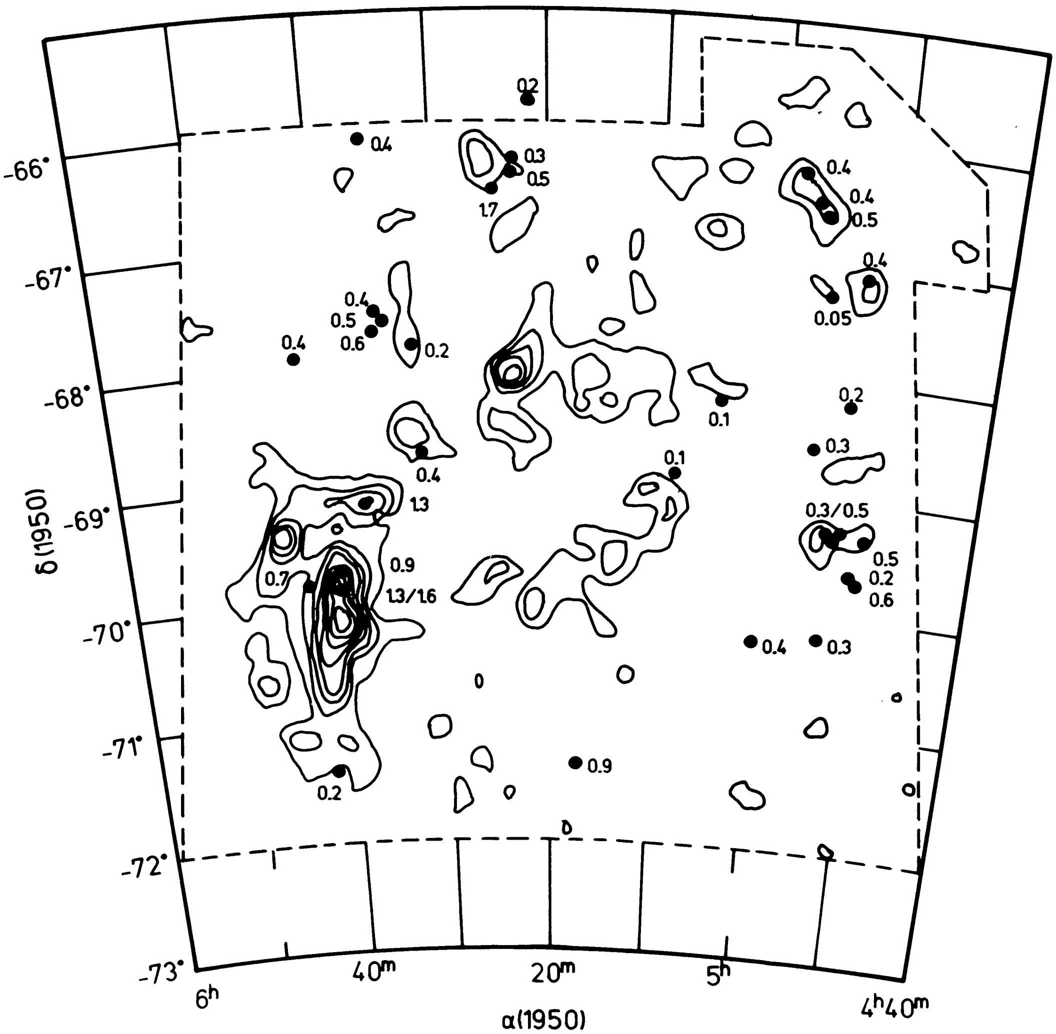

FIGURE 6. — CO map of the LMC (taken from Cohen *et al.*, 1988) with average photometric extinctions superimposed (in mag., corrected for Galactic foreground extinction).